6808–6819 *Nucleic Acids Research, 2007, Vol. 35, No. 20* *Published online 10 October 2007*
doi:10.1093/nar/gkm574

Conserved amino acids in each subunit of the heteroligomeric tRNA m^1A58 Mtase from *Saccharomyces cerevisiae* contribute to tRNA binding

Sarah G. Ozanick[1], Janusz M. Bujnicki[2,3], Daniel S. Sem[4] and James T. Anderson[1,*]

[1]Department of Biological Sciences, Marquette University, P.O. Box 1881, Milwaukee, WI 53201, USA, [2]Laboratory of Bioinformatics and Protein Engineering, International Institute of Molecular and Cell Biology, Warsaw, and [3]Institute of Biotechnology and Molecular Biology, Adam Mickewicz University, Poznan, Poland, and [4]Chemical Proteomics Facility at Marquette, Department of Chemistry, Marquette University, P.O. Box 1881, Milwaukee, WI 53201, USA

Received April 3, 2007; Revised June 28, 2007; Accepted July 13, 2007

ABSTRACT

In *Saccharomyces cerevisiae*, a two-subunit methyltransferase (Mtase) encoded by the essential genes *TRM6* and *TRM61* is responsible for the formation of 1-methyladenosine, a modified nucleoside found at position 58 in tRNA that is critical for the stability of $tRNA_i^{Met}$. The crystal structure of the homotetrameric m^1A58 tRNA Mtase from *Mycobacterium tuberculosis*, TrmI, has been solved and was used as a template to build a model of the yeast m^1A58 tRNA Mtase heterotetramer. We altered amino acids in *TRM6* and *TRM61* that were predicted to be important for the stability of the heteroligomer based on this model. Yeast strains expressing *trm6* and *trm61* mutants exhibited growth phenotypes indicative of reduced m^1A formation. In addition, recombinant mutant enzymes had reduced *in vitro* Mtase activity. We demonstrate that the mutations introduced do not prevent heteroligomer formation and do not disrupt binding of the cofactor S-adenosyl-L-methionine. Instead, amino acid substitutions in either Trm6p or Trm61p destroy the ability of the yeast m^1A58 tRNA Mtase to bind $tRNA_i^{Met}$, indicating that each subunit contributes to tRNA binding and suggesting a structural alteration of the substrate-binding pocket occurs when these mutations are present.

INTRODUCTION

Modified nucleosides are abundant and diverse in transfer RNA (tRNA), and influence translation accuracy (1), reading frame maintenance (2), recognition by aminoacyl-tRNA synthetases (3), and tRNA structure (4). The modifications found in tRNAs occur post-transcriptionally and range from simple base or ribose methylations to more complex multi-step additions (5). Various types of modifications are found throughout a tRNA molecule, but the greatest assortment is found in the anticodon region (6). In most tRNAs from *Saccharomyces cerevisiae*, the modified nucleoside 1-methyladenosine (m^1A) is found at position 58 in the T-loop. This modification results from the transfer of a methyl group from the cofactor S-adenosyl-L-methionine (AdoMet) to the N^1 position of adenosine. While many tRNA modifications are not required for growth, m^1A58 has been found to be essential in yeast (7). Previous work has shown that m^1A58 is necessary to maintain the stability of one tRNA, initiator methionine tRNA ($tRNA_i^{Met}$) (7).

The occurrence of m^1A58 in tRNA is widespread, as it is found in bacterial, archaeal and eukaryotic tRNAs. The tRNA m^1A58 methyltransferase (Mtase) has been characterized in organisms representing each of these domains, and the crystal structure of the *Mycobacterium tuberculosis* tRNA m^1A58 Mtase, TrmI, with AdoMet bound has been solved (8–12). These studies have shown that the bacterial and archaeal tRNA m^1A58 Mtases are composed of one subunit and are found as

*To whom correspondence should be addressed. Tel: +1 414 288 1481; Fax: +1 414 288 7357; Email: james.anderson@mu.edu

homotetramers; however, the known eukaryotic tRNA m^1A58 Mtases consist of two subunits and are believed to function as heterotetramers. In yeast, the two subunits of the tRNA m^1A58 Mtase are encoded by *TRM6* and *TRM61*. Trm61p contains AdoMet-binding motifs and shows obvious and extensive sequence similarity to the bacterial and archaeal tRNA m^1A58 Mtases. *TRM6* has close homologs only in eukaryotic organisms, and does not share evident sequence similarity with any proteins other than orthologs (13). However, based on fold-recognition analyses, it has been postulated that Trm6p and Trm61p have a common core structure, and it has been hypothesized that a duplication of a *trmI*-like ancestral gene, followed by divergent evolution, resulted in the creation of *TRM6* and *TRM61* (13).

There have been only a limited number of studies regarding structure–function relationships in tRNA modification enzymes. Structure–function analyses have been performed for the Mtases responsible for formation of 1-methylguanosine 37 (TrmD) (14), 2′-*O*-methylguanosine 18 (TrmH) (15), and 7-methylguanosine 46 (TrmB) (16), and further insight into the mechanics of these enzymes has been gained from their crystal structures (17–19). However, these enzymes do not have heteroligomeric structures and, as a result, these studies do not give us insight into how Trm6p and Trm61p may interact with each other and a tRNA substrate. Additionally, studies of TrmD and TrmH are not entirely applicable to studies of the m^1A58 Mtase, as these proteins are members of the SPOUT family of Mtases (17,18), while the Trm6p/Trm61p complex is predicted to belong to the larger and structurally distinct Rossmann-fold Mtase family. Lastly, no structure–function studies have been performed for TrmI.

The tRNA m^1A58 Mtase from *S. cerevisiae* is intriguing—tRNA modification enzymes are rarely essential, but *TRM6* and *TRM61* are both essential (20); tRNA Mtases are usually single subunit enzymes, but the yeast tRNA m^1A58 Mtase is composed of two subunits (21), and Rossmann-fold Mtases are mostly monomeric, but Trm6p/Trm61p complexes are oligomeric (22). Because of these peculiarities and our lack of knowledge about this enzyme, we decided to perform a structure–function analysis of the yeast tRNA m^1A58 Mtase. In order to guide our characterization of this enzyme, we created a model of a Trm6p/Trm61p heterotetramer using bioinformatics. Trm6p and Trm61p subunits were modeled individually based on alignments to known TrmI structures obtained by protein fold-recognition analyses. The two subunits were then superimposed onto the structure of the *M. tuberculosis* TrmI homotetramer. Using this model, we introduced mutations into *TRM6* and *TRM61*, targeting conserved amino acids predicted to be important for protein–protein interactions between the subunits of the enzyme. We expected that the resulting mutant enzymes would be defective in Mtase activity due to an inability to form heteroligomers. Surprisingly, the mutations made in Trm6p and Trm61p had no effect on oligomerization and, furthermore, did not inhibit AdoMet binding. Instead, we found that tRNA binding was affected. Loss of tRNA binding resulted from the corresponding homologous mutations in either Trm6p or Trm61p, indicating that both subunits make contributions to protein–substrate interactions. This is the first study to identify the amino acids in a heteroligomeric tRNA Mtase that are required for substrate binding.

MATERIALS AND METHODS

Yeast strains and media

Strain Y350 was created by exchanging the high-copy *LEU2* marked plasmid bearing *IMT4* in strain Y146 (7) for a high-copy *URA3* marked plasmid bearing *IMT4*(C-50) (23). Transformation of yeast strains was done as described (24). Y350 was transformed with YCplac111 (Y351) (25) or the following plasmids described below: p317 (Y353), p326 (Y354), p325 (Y360) or p334 (Y367). Selection for 5-FOA resistance was performed on Sc-leucine plates containing 0.1% 5-FOA. The 5-FOA resistant strains of *trm6-504* (Y361) and *trm6-420* (Y368) were isolated by streaking the initial 5-FOA resistant papillae to another plate containing 5-FOA and waiting for colonies to form. Y261 (*trm61-2*) is strain Hm296 (26). Y261 was transformed with pRS316 (Y428) (27) or the following plasmids described below: pJA148 (Y429), pJA149 (Y430) or p430 (Y431). Gap repair was used to identify the mutation present in the *trm6-504* strain. A plasmid containing *TRM6* (pJA117) was digested with BsrGI and HindIII to create a gap ~500 nt long at the 3′ end of the open reading frame. This plasmid was used to transform strain H2457 (7). Repaired plasmids were isolated and two independent isolates were sequenced. A point mutation was found resulting in a P431R substitution. The BsrGI/HindIII fragment from one of the repaired plasmids was moved into the same sites of pJA117 and used to transform H2457. Transformants failed to complement the temperature sensitive and 3-aminotriazole resistant phenotypes of *trm6-504*, insuring no other mutations were present in *trm6-504*.

Plasmid construction

For expression in yeast, single copy *TRM6* with a histidine/Flag tag was moved from pLPYGCD10His Flag (10) as a SphI/XbaI fragment into the single copy *LEU2* marked plasmid YCplac111 (25) digested with the same enzymes to give p317. Quik Change site-directed mutagenesis (Stratagene) was used to introduce the *trm6-416* (p326), *trm6-504* (p325) and *trm6-420* (p334) mutations into p317. The entire *TRM6* open reading frame in p326 and p334 was sequenced to confirm the presence of the desired mutations and absence of any other mutations. Plasmids carrying *TRM61* (pJA148) and *trm61-3* (pJA149) have been described (10). To create a plasmid carrying *trm61-255*, mutagenesis was performed on *TRM61* in plasmid pAK001 (described below) to give p420. An AgeI/HpaI fragment of *TRM61* containing the *trm61-255* mutation was moved from p420 to AgeI/HpaI digested pJA148 to give p430. The presence of the *trm61-255* mutation was confirmed by DNA sequencing.

For co-expression of *TRM6* and *TRM61* in *Escherichia coli*, both reading frames were initially cloned separately. First, pAK001 was created by inserting a NdeI/BamHI fragment containing *TRM61* with a C-terminal Flag tag into pET11a (Novagen). The NdeI/BamHI fragment came from pJA166, created by PCR amplification of *TRM61* from pJA148 and cloning of the product into pET3a (Novagen). pAK002 was constructed by cloning a NdeI/BamHI fragment containing *TRM6* from pJA165 into pET15b (Novagen) cut with the same enzymes, giving *TRM6* an N-terminal 6×His tag. pJA165 consists of *TRM6*, which was amplified from pMG107 (28) using the PCR and inserted into pET14b (Novagen). The final plasmid for co-expression (p328) was created by inserting a BglII(blunted)/AatII fragment containing *TRM6*-His from pAK002 into pAK001 that had been digested with HindIII(blunted)/AatII. Using Quik Change site-directed mutagenesis (Stratagene), the *trm6-416* (p330), *trm6-504* (p331) and *trm6-420* (p338) mutations were created in p328. The *TRM6* and *TRM61* open reading frames were sequenced to show the presence of the desired mutations and verify that no other mutations had been introduced. The *trm61-3* mutant was created by transferring an AgeI/NheI fragment from pJA149 into p328, producing p358. The *trm61-255* mutant was created by transferring an AgeI/NheI fragment from p420 to AgeI/NheI digested p328 to give p426, and confirmed by DNA sequencing. To create *trm6-416*/*trm61-255*, this same AgeI/NheI fragment was transferred to p330, giving p427, and verified using DNA sequencing. BL21(DE3) cells were transformed with these plasmids to give the following strains used for expression and purification of recombinant Trm6p/Trm61p complexes: *TRM6*/*TRM61* (B329), *trm6-416* (B332), *trm6-504* (B333), *trm6-420* (B343), *trm61-3* (B360), *trm61-255* (B428), *trm6-416*/*trm61-255* (B429).

Structure prediction and protein modeling

(For a detailed description of this process, please see Supplementary Data S1) Fold recognition analyses run via the GeneSilico MetaServer (29) were used to identify the best structural templates. Models of Trm6p and Trm61p subunits, excluding regions of predicted disorder, were built using the 'FRankenstein's monster' approach (30). The model of the Trm6p/Trm61p heterotetramer was constructed by superimposing two copies of Trm6p and Trm61p onto the TrmI homotetramer.

Enzyme purification

Trm6p/Trm61p complexes were purified from *E. coli* using TALON metal affinity resin (Clontech). Cells were grown to OD = 0.2 at 37°C and induced with 0.5 mM IPTG at 30°C for 3 h, then harvested and the pellets frozen at −20°C. Pellets were thawed on ice and resuspended in equilibration buffer (50 mM sodium phosphate, pH 7, 1 M NaCl) with complete protease inhibitor cocktail, EDTA-free (Roche). After sonication and centrifugation (12 000*g*, 20 min, 4°C), clarified cell extract was incubated at 4°C for 2 h with TALON resin in equilibration buffer. Enzyme purification was carried out at 4°C following the manufacturer's instructions for batch/gravity-flow column purification, using 20 mM imidazole in wash buffer and 200 mM imidazole in elution buffer.

In vitro activity assays

Mtase activity assays of purified enzymes were conducted as described (10,11) using Mtase buffer (100 mM Tris, pH 7.6/0.1 mM EDTA/10 mM $MgCl_2$/100 mM NH_4Cl/1 mM DTT). A standard assay contained 15 nM enzyme, 150 nM *in vitro* transcribed $tRNA_i^{Met}$ (11), and 30 μM S-adenosyl-L-[methyl-^{3}H]methionine (GE Healthcare). The amount of radioactivity incorporated into $tRNA_i^{Met}$ was determined by first collecting the acid-insoluble material from the reaction on a GN-6 metricel membrane disc filter (Pall) using a vacuum manifold, and then quantitating the radioactivity on the filter using liquid scintillation counting.

Gel filtration chromatography

To analyze Trm6/Trm61p complexes from yeast, cells were washed with 1 × Tris buffered saline (TBS) (31), resuspended in breaking buffer [1 × TBS, 1 mM DTT, 1 × complete protease inhibitor cocktail (Roche)], and lysed using a French press. Cell extract was subjected to centrifugation (107 000*g*, 1 h, 4°C) and the clarified extract injected onto a Superose 12 HR 10/30 column (GE Healthcare) equilibrated with 1 × TBS. The fractions collected from the column were precipitated with acetone, subjected to SDS-PAGE, and transferred to nitrocellulose for western blotting. Protein standards (Sigma) were analyzed similarly, but were not precipitated and were detected by Coomassie blue staining. Antibodies to either Trm6p or Trm61p were used to visualize the elution patterns of the proteins by immunoblot analysis.

Recombinant enzyme from *E. coli*, purified as described above, was also analyzed using gel filtration. Purified enzyme (200 μg) in elution buffer (50 mM sodium phosphate, pH 7, 1 M NaCl, 200 mM imidazole) was injected onto a Superose 12 HR 10/30 column (GE Healthcare) equilibrated with 50 mM sodium phosphate, pH 7, 1 M NaCl. Proteins recovered in the fractions collected from the column were separated by SDS-PAGE and visualized using Coomassie blue staining. Protein standards (Sigma) were analyzed in the same way.

STD-NMR spectroscopy

Purified recombinant enzymes were exchanged into an NMR buffer comprised of 20 mM sodium phosphate, pH 7.0 (uncorrected for isotope effect) and 200 mM NaCl in D_2O, using PD-10 gel filtration columns (GE Healthcare). Saturation transfer difference (STD) spectra of enzymes at 7 μM were obtained on a 600 MHz Varian NMR System at 8°C using the cyclenoe program (Varian pulse sequence), with low power (−6 dB) irradiation performed for 4 s using a train of 100 ms rectangular pulses. Two interleaved spectra were obtained, one with irradiation of upfield shifted protein methyl resonances (at 0 p.p.m.) and a second control spectrum with off-resonance irradiation at −10 p.p.m., and these spectra were subtracted to give the STD spectrum. AdoMet

signals that were monitored included resonances at 6 p.p.m. (ribose) and 8.2 p.p.m. (adenine ring), which were well-resolved from residual protein signals. Control STD experiments were done in the absence of protein or in the absence of AdoMet, and they gave no false positive STD signals. Enzymes (wt or mutant) were titrated with 0, 100, 200, 300, 400, 600 or 800 μM AdoMet by repeated addition of AdoMet immediately before performing the STD experiment (acquisition time = 1 h, 512 acquisitions). All spectra were printed with the same vertical scale and the height of the resonance for an adenine ring proton of AdoMet was measured for the STD signal. Data were fitted to Equation (1) using SigmaPlot (Systat):

$$\mathrm{STD} = \mathrm{STD}_{\max} - (\mathrm{STD}_{\max})/(1 + [\mathrm{AdoMet}]/K_{\mathrm{d}}) \quad \mathbf{1}$$

where STD is the intensity change for AdoMet protons, at a given AdoMet concentration ([AdoMet]), $\mathrm{STD}_{\max}$ is the corresponding signal when enzyme is fully bound with AdoMet and K_{d} is the dissociation constant for AdoMet binding to enzyme. STD signals were effectively adjusted with the amplification factor (32). Errors for the fitted K_{d} values represent SDs from the nonlinear least squares fitting process.

tRNA-binding assays

tRNA binding was studied by incubating 500 nM enzyme with ~1 nM ^{32}P end-labeled $\mathrm{tRNA_i^{Met}}$ in Mtase buffer in a total volume of 20 μl. The $\mathrm{tRNA_i^{Met}}$ used was previously purified from a *trm6Δ* strain (Y146) (10). Reactions were incubated for 20 min at room temperature and then put on ice for 5 min. $\mathrm{tRNA_i^{Met}}$ bound to Trm6p/Trm61p was collected on a GN-6 metricel membrane disc filter (Pall) using a vacuum manifold. Filters were washed with Mtase buffer, dried and counted by liquid scintillation. To determine the K_{d} of the wild-type enzyme, 1 nM ^{32}P end-labeled $\mathrm{tRNA_i^{Met}}$ was incubated with 50 nM, 100 nM, 250 nM, 500 nM, 1 μM, 5 μM or 10 μM enzyme and the assay carried out as described above. The K_{d} value was obtained by performing a nonlinear least squares fit of the data using SigmaPlot (Systat).

RESULTS

Trm6/Trm61p heterotetramer modeling

To provide a structural platform for sequence–function analyses, we decided to construct a model of the Trm6p/Trm61p enzyme using bioinformatics. First, the Protein Data Bank was searched with the Trm6p and Trm61p sequences to find close homologs that could serve as modeling templates. We ran a set of fold-recognition (FR) methods via the GeneSilico MetaServer (29) to obtain target-template alignments. The best structural templates reported by the FR methods for both Trm6p and Trm61p were the prokaryotic TrmI family members from *M. tuberculosis* (1i9g) and *Thermotoga maritima* (1o54). An alignment of these templates with Trm6p and Trm61p reveals long insertions and terminal extensions in Trm6p and Trm61p (60–185, 308–339 and 450–478 in Trm6p and 1–11, 266–342 and 370–384 in Trm61p) that are not present in prokaryotic homologs (Figure 1A) and algorithms for disorder prediction suggested these regions are flexible and lack a defined 3D structure. The alignment also illustrates that many of the residues predicted to be important for tetramer formation in TrmI, such as E229, R233, W235 and P244, are conserved in the two eukaryotic proteins (highlighted in Figure 1A). Importantly, these residues are located in the same positions in our Trm6p/Trm61p tetramer model as in the TrmI structure.

Based on the crystal structure of TrmI, salt bridges between residues E229 and R233 from each subunit are predicted to provide crucial strength for the tetramer (12). As these residues are highly conserved in the entire $\mathrm{m^1A}$ Mtase family, including both *TRM6* and *TRM61* in yeast (E416 and R420 in Trm6p; E255 and R259 in Trm61p, Figure 1A), we hypothesized that these amino acids may play an important role in formation or stabilization of quaternary structure (Figure 1B and Figure S1). The crystal structure of TrmI also shows that W235, P244 and H251 form a three-layer sandwich, comprised of W235 and P244 from one subunit and H251 from another, that may contribute to the stability of the homotetramer. In both human and yeast Trm6p and Trm61p, as well as many other organisms, the aromatic nature of W235 is conserved by the presence of tyrosine (Y422 in Trm6p and Y261 in Trm61p); therefore, we predicted this amino acid may also be important for the stability of the eukaryotic heteroligomer (Figure 1B and Figure S1). While P244 is not conserved in Trm61p (substituted by methionine), it is conserved in Trm6p (P431); conversely, H251 is conserved in Trm61p (H354), but not in Trm6p (substituted by glycine). The preservation of this H–P pair suggested that it may contribute to the stability of the interface between subunits (Figure 1B and Figure S1).

In order to study the role of these conserved amino acids in yeast Trm6p/Trm61p protein–protein interactions, we introduced alanine substitutions to remove side chains. The Trm6p mutants created are *trm6-416*, which has alanine substitutions at positions E416, R420 and Y422, and *trm6-420*, which has an alanine substitution at position R420 (Table 1). A spontaneous Trm6p mutant that was previously isolated, *trm6-504* (33), was also included in these studies because we found that this mutant has an arginine substitution at P431. A Trm61p mutant was also created with mutations corresponding to those of *trm6-416*. This mutant, *trm61-255*, has alanine substitutions at E255, R259 and Y261 (Figure 1A). Finally, the mutations in *trm6-416* and *trm61-255* were combined to create *trm6-416*/*trm61-255* (Table 1).

Mutations in *TRM6* and *TRM61* result in growth defects

Although *TRM6* is an essential gene, a *trm6* deletion (*trm6Δ*) strain is viable when a high-copy plasmid containing *IMT4*, which encodes $\mathrm{tRNA_i^{Met}}$, is present (7). To demonstrate whether or not mutations in Trm6p affect $\mathrm{m^1A58}$ Mtase activity, a *trm6Δ* strain that overexpresses $\mathrm{tRNA_i^{Met}}$ from a plasmid marked with *URA3* (Y350) was transformed with a single copy *LEU2* marked plasmid containing either *TRM6* (Y353),

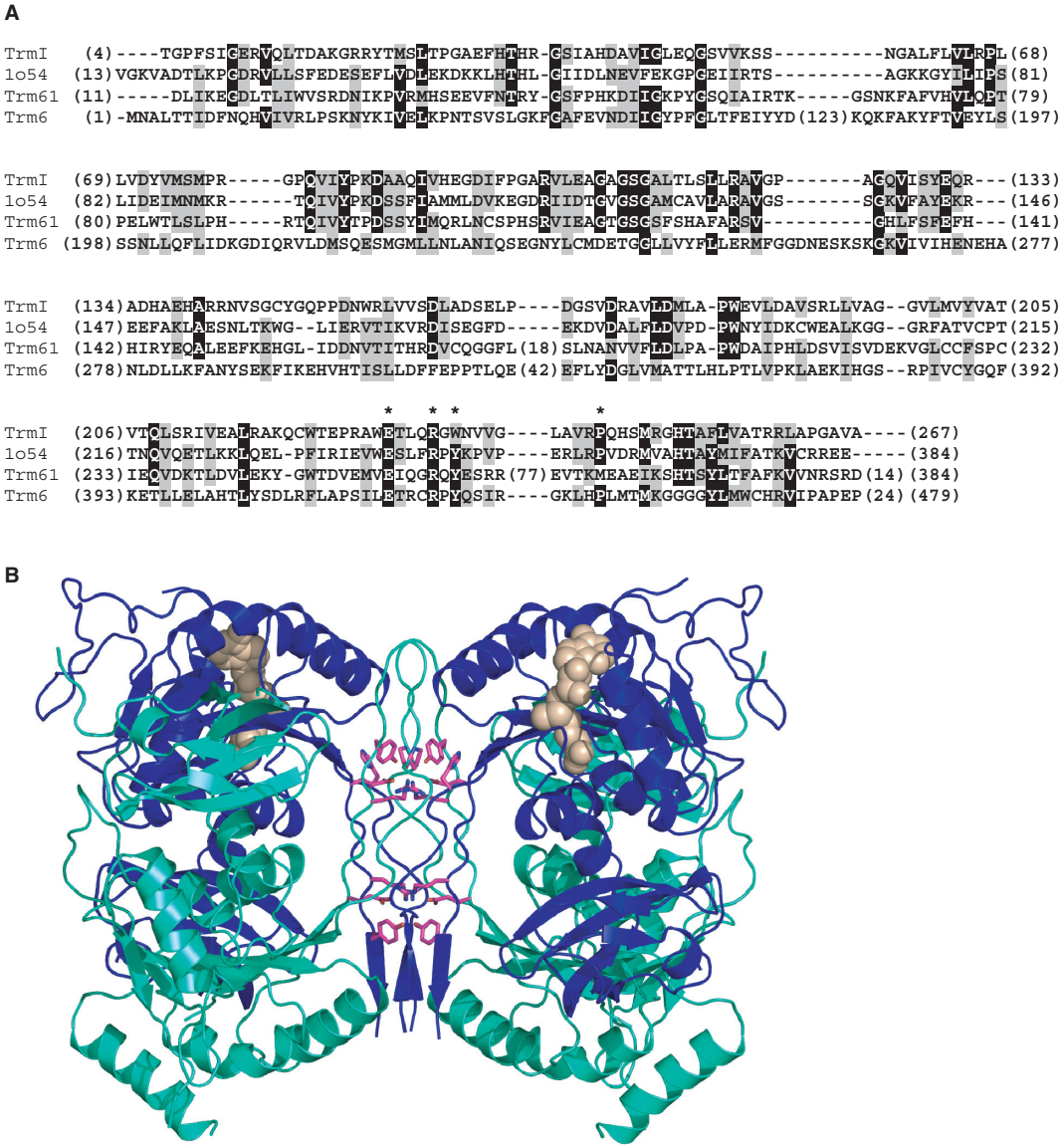

Figure 1. Modeling templates and predicted structure of the Trm6p/Trm61p tetramer. (**A**) Modeling templates aligned with Trm6p and Trm61p sequences. The shaded background designates chemically similar residues while the black background designates identical residues among at least three sequences. Residues mutated in this study (E416, R420, Y422 and P431 in Trm6p and E255, R259 and Y261 in Trm61p) are indicated by asterisks. TrmI is the m^1A58 Mtase from *M. tuberculosis*. 1o54 is a predicted AdoMet-dependent Mtase from *T. maritima*. (**B**) The predicted Trm6p/Trm61p tetramer is shown with Trm6 subunits in teal and Trm61p subunits in blue. AdoMet (tan, spacefill) is shown bound to both Trm61p subunits. The amino acids that were mutated in this study (E416, R420, Y422 and P431 in Trm6p and E255, R259 and Y261 in Trm61p) are shown with side chains in fuchsia. Flexible loops lacking defined structure are not shown. Figure generated with PyMOL (41).

Table 1. *trm6/61* mutants constructed

Mutant	Amino acid substitutions
trm6-416	E416A, R420A, Y422A
trm6-420	R420A
trm6-504	P431R
trm61-3	G118A, G120A
trm61-255	E255A, R259A, Y261A
trm6-416/trm61-255	E416A, R420A, Y422A, E255A, R259A, Y261A

trm6-416 (Y354), *trm6-504* (Y360) or *trm6-420* (Y367). Expression of Trm6p was found to be similar between the wild-type and mutant strains (data not shown). These strains were then evaluated on plates containing 5-fluoroorotic acid (5-FOA), which selects against *URA3*. Patches of cells grown on synthetic complete media lacking uracil and leucine (Sc-ura-leu) were replica printed to Sc-leu plates containing 5-FOA. Under these conditions, expression of *TRM6* permitted growth throughout the patch, indicating the *URA3* marked plasmid encoding $tRNA_i^{Met}$ had been readily evicted from these cells (Figure 2A). The strains expressing

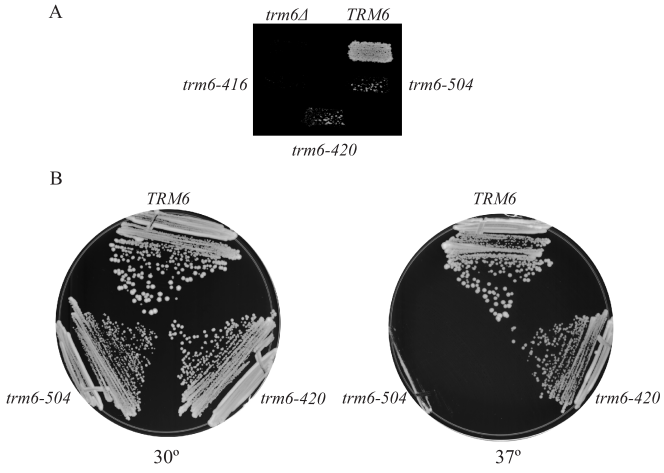

Figure 2. *trm6* mutants exhibit growth defects. (**A**) A *trm6Δ* strain over-expressing $tRNA_i^{Met}$ and containing empty vector (Y351) or single copy *TRM6* (Y353), *trm6-416* (Y354), *trm6-504* (Y360) or *trm6-420* (Y367) was patched to a Sc-leu plate, grown, replica printed to a Sc-leu plate containing 5-FOA and incubated at 30°C for 3 days. (**B**) *trm6-420* and *trm6-504* strains that evicted the high-copy *IMT4* plasmid (Y368 and Y361, respectively) were grown on YPD (Yeast extract/Peptone/Dextrose) at either 30 or 37°C for 3 days.

trm6-504 and *trm6-420* were able to form papillae, but not a confluent patch, indicating only occasional eviction of the *URA3* plasmid. The *trm6-416* strain and the *trm6Δ* strain carrying an empty vector (Y351) were unable to grow (Figure 2A). The growth of cells containing *TRM6* is expected because a functional m^1A58 Mtase would be present and over-expression of $tRNA_i^{Met}$ would no longer be required. The limited growth of the *trm6-504* and *trm6-420* mutants suggests the m^1A58 Mtase has reduced activity, while the complete lack of growth of the *trm6-416* strain suggests the enzyme is no longer functional. The phenotypes observed using 5-FOA selection were the first indication that the mutations created in Trm6p had a detrimental effect on m^1A58 Mtase activity.

It has been previously noted that a *trm6-504* mutant strain is temperature-sensitive (Ts^-) at 37°C due to decreased levels of mature $tRNA_i^{Met}$, thought to result from a decrease in the stability of $tRNA_i^{Met}$ tertiary structure from the absence of m^1A58 (7,33). Because the Ts^- phenotype can serve as a measure of mature $tRNA_i^{Met}$ levels in *trm6* mutant strains, the 5-FOA resistant cells containing *trm6-504* (Y361) or *trm6-420* (Y368) were tested for temperature sensitivity. The *trm6-420* strain exhibited slow growth at 30 and 37°C, while the *trm6-504* displayed slow growth at 30°C and a Ts^- phenotype at 37°C (Figure 2B). This result suggests that the *trm6-504* and *trm6-420* strains have reduced amounts of mature $tRNA_i^{Met}$, presumably due to decreased m^1A58 Mtase activity.

Because the three amino acids mutated in *trm6-416* are also found in a topologically similar position in Trm61p, we created a Trm61p mutant with the corresponding mutations to see if these amino acids were also important for activity. This mutant, *trm61-255*, was tested for its ability to complement a *trm61-2* strain (Y261), which has a temperature-sensitive phenotype (26,34). The *trm61-2* strain was transformed with an empty plasmid (Y428) or the same plasmid carrying either *TRM61* (Y429), *trm61-255* (Y431) or *trm61-3* (Y430). The *trm61-3* mutant has two conserved glycine residues in its predicted AdoMet-binding motif changed to alanines, causing a null mutant by inactivating the enzyme (10). Only expression of *TRM61* was able to complement the growth defect of the *trm61-2* strain (data not shown), suggesting that Trm61-255p does not form an active m^1A58 Mtase in the presence of Trm6p. We conclude from these studies that the conserved sequence of E, R and Y residues in both the Trm6p and Trm61p subunits is crucial for Mtase activity.

Mutations in Trm6p result in reduced m^1A Mtase activity *in vivo* and *in vitro*

The growth phenotypes described above suggest that Trm6-416p, Trm6-420p and Trm6-504p cannot form fully functional m^1A58 Mtases in the presence of Trm61p. To confirm that tRNA from these strains was lacking m^1A, we used high performance liquid chromatography (HPLC) to determine the modified nucleoside content of total tRNA from a *trm6Δ* strain over-expressing $tRNA_i^{Met}$ and containing single copy *TRM6* (Y353), *trm6-416* (Y354), *trm6-504* (Y360), *trm6-420* (Y367) or empty vector (Y351) (Figure 3). In order to control for the amount of sample loaded onto the HPLC column, modified nucleoside levels in each sample were normalized to the amount of pseudouridine (Ψ) detected in that sample. Ψ was used for this purpose as it is a modified nucleoside and its formation does not depend on the presence of m^1A58 in tRNA (35). The amount of m^1A or Ψ detected was determined using the area of the peak from the HPLC chromatogram. In contrast to the equivalent levels of the modified nucleoside N^2, N^2-dimethylguanosine detected in all samples (data not shown), the *trm6* mutants contained reduced levels of m^1A (Figure 3). The m^1A levels in the *trm6* mutants are reported as a percentage of the amount found in the *TRM6* strain, which was set to 100%. The level of m^1A was lowest in the *trm6-416* strain, which had only 5% of the amount found in the *TRM6* strain, while the *trm6-420* and *trm6-504* strains contained greater amounts of m^1A, 35 and 19%, respectively (Figure 3). The HPLC data supports our interpretation of the growth studies, illustrating that the *trm6* mutants have reduced m^1A Mtase activity *in vivo*. In addition, the magnitude of the growth defects seen for the mutant strains are mirrored by the m^1A levels, as the lowest levels of m^1A are found in the strains with the most severe growth defects.

In order to produce large quantities of mutant enzymes and be able to combine mutations in both Trm6p and Trm61p, we reconstructed each *trm6* mutant in a vector that allows co-expression of *TRM6* and *TRM61* in bacteria. *TRM61* was expressed in *E. coli* together with either *TRM6* (B329), *trm6-416* (B332), *trm6-420* (B343) or *trm6-504* (B333). Using a polyhistidine tag on Trm6p, protein was purified from soluble *E. coli* extract using affinity chromatography. Trm61p co-purified with

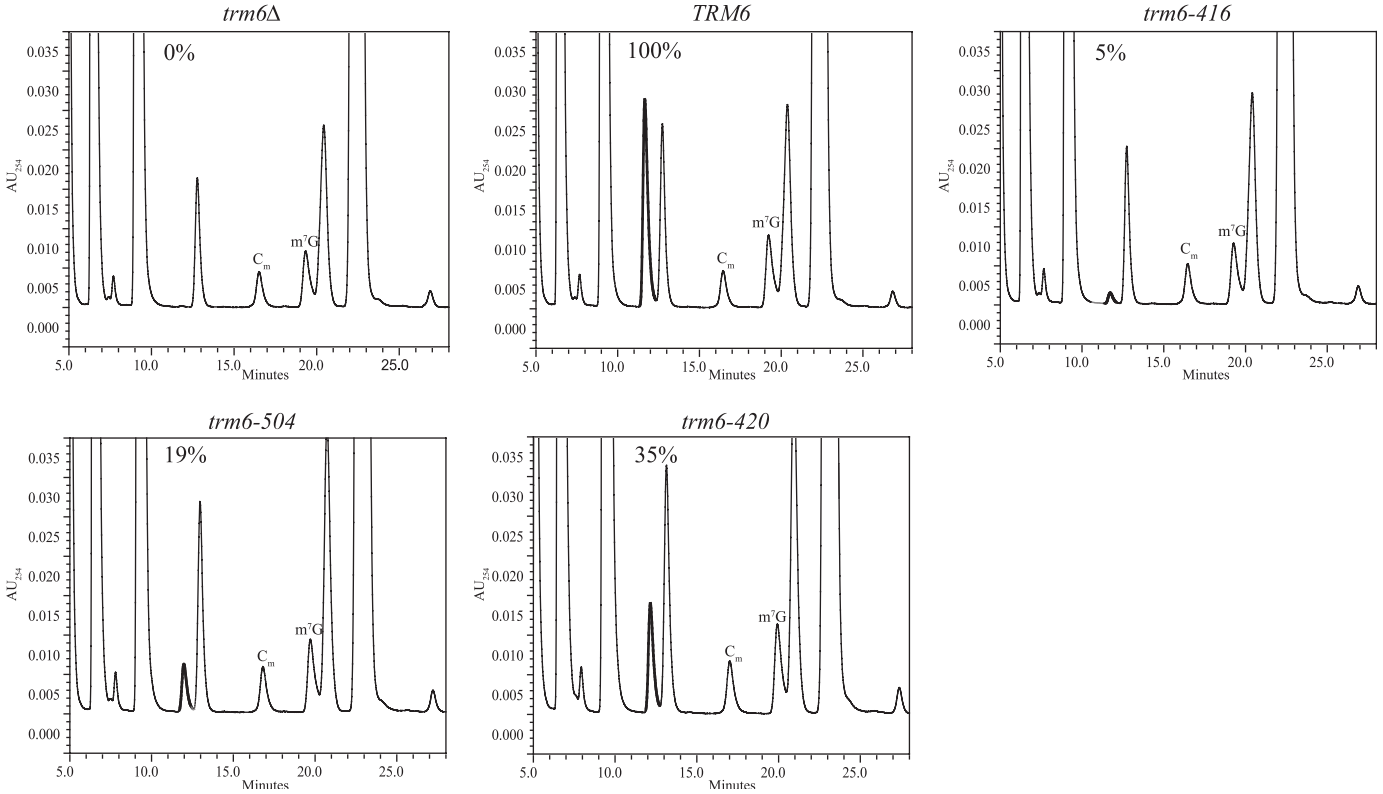

Figure 3. *trm6* mutant strains have reduced levels of m^1A in tRNA. Total tRNA purified from a *trm6Δ* strain over-expressing $tRNA_i^{Met}$ and containing empty vector (Y351) or single copy *TRM6* (Y353), *trm6-416* (Y354), *trm6-504* (Y360) or *trm6-420* (Y367) was digested to single nucleotides and analyzed by HPLC as described previously (7). The absorbance at 254 nm (AU_{254}) was measured and the portion of the chromatogram where m^1A elutes is shown plotted against the retention time in minutes. The peak corresponding to m^1A is bold and the percent of m^1A, as compared to the *TRM6* strain, which was set to 100%, is listed. For each sample, the amount of m^1A detected was normalized to the amount of pseudouridine detected. Peaks corresponding to 2′-*O*-methylcytidine (C_m) and 7-methylguanosine (m^7G) are labeled for reference.

both wild-type Trm6p and Trm6-416p, Trm6-420p and Trm6-504p in apparent stoichiometric amounts (Figure 4A). Purified recombinant enzymes were incubated with S-adenosyl-L-[methyl-^{3}H]methionine (^{3}H-AdoMet) and *in vitro* transcribed $tRNA_i^{Met}$. The incorporation of ^{3}H into $tRNA_i^{Met}$ was monitored by liquid scintillation counting. Under optimal conditions, the wild-type enzyme has been found to convert a maximum of 50% of tRNA substrate to product. In the assays reported in this study, for which the results are shown as the counts per minute of ^{3}H detected, the wild-type enzyme converted ~40% of substrate to product, but the mutant enzymes lacked Mtase activity (Figure 4B). Since the *trm61-3* and *trm61-255* mutants were not able to complement a *trm61-2* strain, we also reconstructed these mutants and co-expressed them in bacteria with *TRM6* (B360 and B428, respectively). In addition, we created a mutant, called *trm6-416*/*trm61-255* (B429), which has the three mutations in *trm6-416* combined with the three mutations in *trm61-255*. All of these enzymes also lacked *in vitro* Mtase activity (Figure 4B).

While we did not observe *in vitro* Mtase activity for the *trm6-420* and *trm6-504* mutants, the HPLC analysis of tRNA from yeast expressing these Trm6p mutants had shown some m^1A was still formed *in vivo*, although far less efficiently than wild-type enzyme (Figure 4B). Therefore, we suspected that the low level of activity of these mutants was undetectable in our *in vitro* assay or indistinguishable from a negative control. Therefore, we increased the concentration of enzyme and tRNA in the assay 10-fold to try and amplify the signal-to-noise ratio and make low-level activity detectable. Under these conditions, the *trm6-504* and *trm6-420* mutant enzymes consistently showed Mtase activity (Figure 4B). Trm6p-420/Trm61p complexes consistently displayed more potent Mtase activity than the other Trm6p mutants, in accord with the less severe growth defect and higher level of m^1A seen in yeast expressing this mutant.

Mutations in Trm6p and Trm61p do not prevent heteroligomer formation

Based on its crystal structure, the m^1A58 Mtase from *M. tuberculosis* was described as a dimer of two dimers (12). The interactions between the two subunits that form one dimer are extensive, while the interactions between all four subunits are limited to a central barrel structure (12). As described above, we created alanine substitutions in Trm6p and Trm61p in order to destabilize protein–protein interactions and found that the mutant enzymes had reduced Mtase activity, although all of the mutant

A.

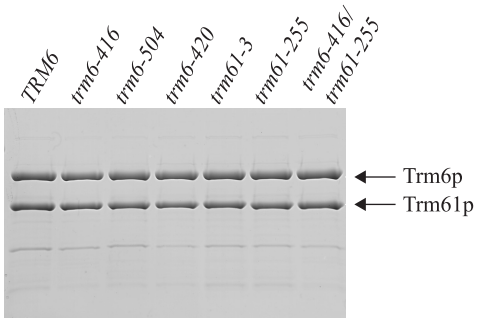

B

TRM6/61 Allele:	Standard reaction (counts/min.^{3}H)	10X Reaction (counts/min.^{3}H)
TRM6	2,542	26,352
trm6-416	69	147
trm6-504	98	232
trm6-420	80	598
trm61-3	64	220
trm61-255	64	62
trm6-416/trm61-255	57	88
No Enzyme	62	167

Figure 4. Purification and characterization of recombinant Trm6p/Trm61p complexes. **(A)** Wild-type and mutant enzymes were purified from *E. coli* whole cell extract via a polyhistidine tag on Trm6p. Samples were analyzed by SDS-PAGE and stained with Coomassie blue. (**B**) Fifteen nanomolar of purified recombinant enzyme was incubated with 30 μM ^{3}H-AdoMet and 150 nM *in vitro* transcribed $tRNA_i^{Met}$ (standard reaction), or 150 nM enzyme was incubated with 30 μM ^{3}H-AdoMet and 1.5 μM $tRNA_i^{Met}$ (10 × reaction). After precipitation with 5% trichloroacetic acid, insoluble material was collected on nitrocellulose filters and ^{3}H was measured using liquid scintillation. The data reported is the average of duplicate experiments.

enzymes were still capable of forming heterodimers (Figure 4A). We wanted to determine whether this loss of activity was due to disruption of the predicted heterotetrameric structure of the enzyme. To size mutant Trm6p/Trm61p complexes, purified recombinant enzyme was analyzed by gel filtration chromatography. The fractions that contained Trm6p and Trm61p were determined using SDS-PAGE followed by Coomassie blue staining. Since the molecular weight of Trm6p is 55 kDa, and that of Trm61p is 44 kDa, a heterotetramer would be ~200 kDa. The elution pattern of Trm6p/Trm61p complexes was consistent with formation of a hetero-ligomer, possibly a heterotetramer. Furthermore, no differences were seen between the elution profiles of the wild-type and *trm6-416*, *trm6-420* and *trm6-504* enzymes (data not shown), which led us to hypothesize that the substitutions in the Trm6p mutants were not enough to destabilize the predicted tetramer because other interactions provided by amino acids on Trm61p remained intact. Therefore, we also analyzed the *trm61-255* mutant and the *trm6-416*/*trm61-255* double mutant. We purified recombinant wild-type and Trm6-416p/Trm61p, Trm6p/Trm61-255p and Trm6-416p/Trm61-255p mutant complexes and used gel filtration chromatography to determine the sizes of these enzymes. All three mutant enzymes fractionated the same as the wild-type enzyme (Figure 5A). In conclusion, none of the mutations made in Trm6p and Trm61p to the predicted protein–protein interface of the yeast Mtase disrupted oligomerization.

To be confident that the results obtained using recombinant purified enzymes reflected the structure of the enzyme in yeast, gel filtration chromatography was also performed using soluble whole cell extract from yeast strains expressing either *TRM6* (Y353), *trm6-416* (Y354), *trm6-504* (Y360) or *trm6-420* (Y367). The fractions collected from the gel filtration column were subjected to SDS-PAGE and western blotting to visualize Trm6p and Trm61p. Again, the wild-type and mutant enzymes were found to have the same elution patterns (Figure 5B). In addition to gel filtration chromatography, limited proteolysis was used to try to detect structural differences between wild-type and mutant enzymes. After digestion of the wild-type and *trm6-416*, *trm6-420*, *trm6-504*, *trm61-3*, *trm61-255 and trm6-416*/*trm61-255* enzymes with non-specific proteases for set periods of time, no differences in the cleavage pattern and rate were observed between wild-type and mutant complexes (data not shown). Overall, these experiments imply that alteration of conserved amino acids predicted to be involved in protein–protein interactions do not prevent oligomerization or cause drastic changes in the overall structure of the yeast m^1A58 Mtase. Therefore, the reduced Mtase activity observed is the result of a different defect caused by the mutations—such as loss of either substrate or co-factor binding.

Trm6p mutants are not defective for AdoMet binding

Previously, it was noted that *TRM61* contains binding motifs for AdoMet (34), and later it was found that mutation of two conserved glycine residues in motif I destroys Mtase activity (10). However, *TRM6* does not have these motifs; therefore, we did not expect the mutations present in *trm6-416*, *trm6-420* and *trm6-504* to affect AdoMet binding. Nevertheless, we wished to eliminate this as a possible reason for the reduced activity observed for these mutants, and used a ligand-binding assay which does not rely on enzymatic activity. To this end, saturation transfer difference-nuclear magnetic resonance (STD-NMR) spectroscopy was used to measure AdoMet binding to protein. STD-NMR is able to measure binding to a protein, based on transfer of magnetization from protein (which is irradiated with R_f energy) to any ligand that comes into contact with the protein (32,36,37). The STD signal that is measured increases in proportion to the fractional saturation of protein-binding sites with ligand. Using this method, AdoMet binding was detected when magnetization was transferred from irradiated purified protein to AdoMet. Control STD spectra collected when the protein was not irradiated were subtracted from those obtained when the protein was irradiated, so that the resulting STD spectrum would reflect only AdoMet molecules that had been in contact with the protein. The resonances corresponding to AdoMet protons were identified based on known ^{1}H NMR chemical shifts (38). Recombinant purified enzymes were incubated with a range of AdoMet concentrations

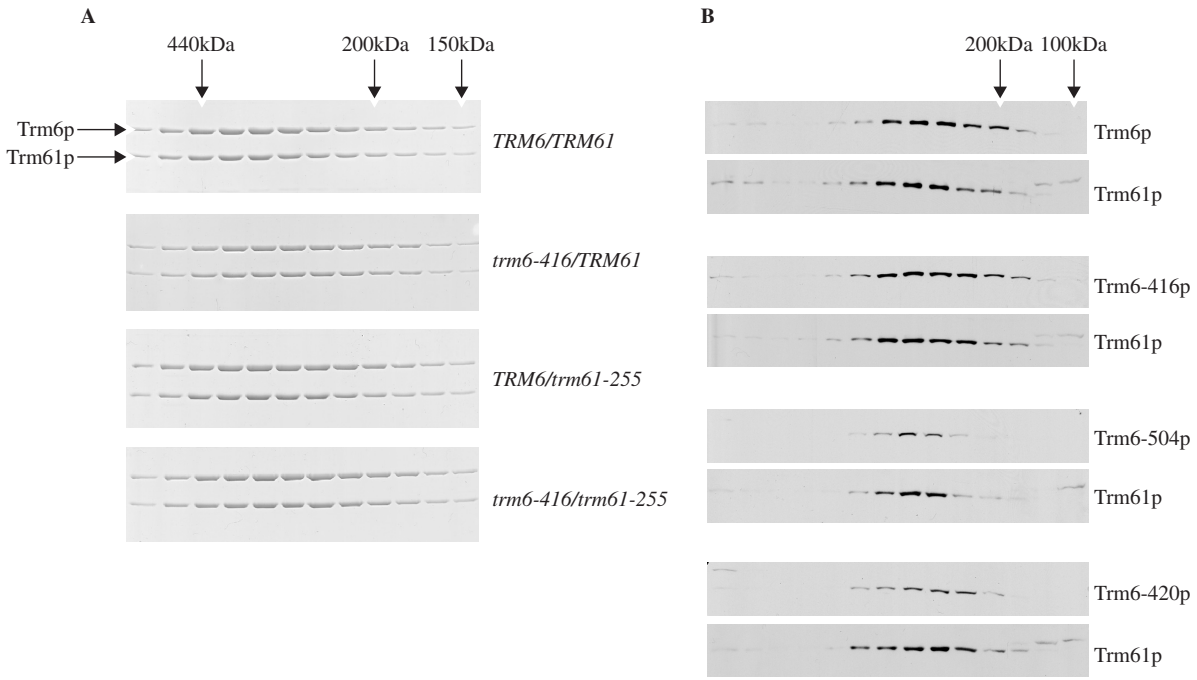

Figure 5. Mutations in Trm6p and Trm61p do not prevent oligomerization. (**A**). Purified recombinant enzymes were fractionated using Superose 12 gel filtration chromatography and visualized using SDS-PAGE followed by Coomassie blue staining. (**B**) Whole cell yeast extract from a strain expressing either *TRM6* (Y353), *trm6-416* (Y354), *trm6-504* (Y360) or *trm6-420* (Y367) was fractionated using Superose 12 gel filtration chromatography. Fractions were analyzed using SDS-PAGE followed by western blotting with antibodies to either Trm6p or Trm61p. Positions of molecular weight standards (Apoferritin, 443 kDa; β-Amylase, 200 kDa; Alcohol Dehydrogenase, 150 kDa; Phosphorylase b, 100 kDa) are indicated along the top of the figures.

Table 2. AdoMet K_d values

TRM6/61 Allele	K_d (μM)
TRM6	376 ± 73
trm6-416	634 ± 73
trm6-504	206 ± 35
trm61-3	ND*

*ND: The K_d value could not be determined as only very low levels of binding were seen at the highest concentrations of AdoMet tested.

and then subjected to STD-NMR spectroscopy in order to generate a binding curve and an estimated K_d (see Materials and Methods section) For wild-type enzyme, the K_d was found to be 376 ± 73 μM (Table 2). The K_d values obtained for the mutant enzymes were not considerably different, at 206 ± 35 μM for *trm6-504* and 634 ± 73 μM for *trm6-416* (Table 2). *trm6-420* was not tested because the mutation present in *trm6-420* is also found in *trm6-416*. As a control for defective AdoMet binding, the predicted AdoMet-binding mutant *trm61-3* was also tested. Trm6p/Trm61-3p complexes showed weak AdoMet binding only at the highest concentrations of AdoMet tested (800 μM), so a K_d value could not be determined. This result not only validates the specificity of the STD-NMR assay, but also suggests that only Trm61p is responsible for AdoMet binding, as AdoMet was not bound even though wild-type Trm6p was present.

tRNA binding is diminished in Trm6p and Trm61p mutants

Because mutations made in Trm6p that are predicted to be located at the Trm6p/Trm61p interface did not affect oligomerization or AdoMet binding, we wanted to determine whether or not tRNA binding was altered. First, increasing amounts of purified recombinant wild-type enzyme were incubated with radiolabeled $tRNA_i^{Met}$ purified from a *trm6Δ* strain (Y146) (7). $tRNA_i^{Met}$ bound by Trm6p/Trm61p complexes was trapped on a nitrocellulose filter and quantitated by liquid scintillation counting. A binding curve generated from this data (Figure 6A) was used to determine the K_d for tRNA to be 330 ± 80 nM. To test the tRNA-binding ability of *trm6* mutant enzymes, purified enzymes (500 nM) were assayed as described above. The *trm6-416*, *trm6-420* and *trm6-504* mutants did not bind considerably more tRNA than a control reaction lacking enzyme (Figure 6B). In addition, we did not detect tRNA binding when the concentration of *trm6-416* and *trm6-420* complexes used was increased 10-fold (5 μM), and, therefore, could not create binding curves for these enzymes. Because the mutations in *trm61-255* and *trm6-416/trm61-255* are predicted to lie in a structurally similar region as the *trm6* mutations, and as these enzymes form oligomers but lack activity, we tested their ability to bind tRNA. Similar to *trm6-416*, *trm6-420* and *trm6-504* mutants, the *trm61-255* and *trm6-416/trm61-255* mutants did not bind $tRNA_i^{Met}$ (Figure 6B). Importantly, the *trm61-3* mutant, which we have shown is defective in AdoMet binding, is able to bind $tRNA_i^{Met}$ as effectively as the wild-type

A

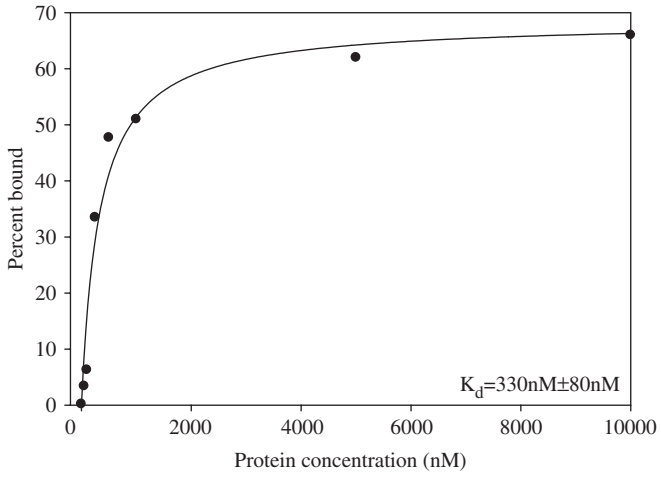

B

TRM6/61 Allele:	Percent bound:
TRM6	100
trm6-416	3
trm6-504	4
trm6-420	4
trm61-3	102
trm61-255	3
trm6-416/trm61-255	3
No Enzyme	1

Figure 6. Mutations in either Trm6p or Trm61p abolish tRNA binding. (**A**) Various concentrations of purified recombinant wild-type enzyme were incubated with a constant amount of ^{32}P end-labeled $tRNA_i^{Met}$ (1 nM) purified from a *trm6Δ* strain (Y146) (7). Bound $tRNA_i^{Met}$ was trapped on a nitrocellulose filter and measured using liquid scintillation. The percent bound was determined by dividing the amount of radiolabeled tRNA bound by the total amount of radiolabeled tRNA in each reaction. (**B**) Purified recombinant wild-type and mutant enzymes were tested for tRNA binding as in (A), but with 500 nM protein. The percent $tRNA_i^{Met}$ bound is reported as a percentage of that bound by the wild-type enzyme, which was set to 100%, corresponding to ~30% of the input bound. The data reported is the average of duplicate trials.

enzyme. We conclude that the reduced m^1A levels observed *in vivo* and the lack of Mtase activity seen *in vitro* result from the inability of *trm6-416*, *trm6-420*, *trm6-504*, *trm61-255* and *trm6-416*|*trm61-255* mutants to effectively bind their tRNA substrate.

DISCUSSION

Because of the lack of information that currently exists regarding structure–function relationships of heteroligomeric tRNA Mtases, we have performed a structure–function analysis of the yeast m^1A58 Mtase using a model we created as a guide. We designed a set of mutations of residues predicted to be involved in protein–protein interactions in Trm6p and Trm61p that are also conserved in TrmI, and evaluated the effects of these mutations on enzyme function. Although we predicted these mutations would destabilize the interactions between the subunits, all mutants retained the ability to form heteroligomers, even a variant with three substitutions in Trm6p (E416A, R420A and Y422A) and three substitutions in Trm61p (E255A, R259A and Y261A), i.e. a protein that lacked 12 functional groups in the protein–protein interface (Figure 1B and Figure S1). We then tested two *trm6* mutants to see if AdoMet binding was affected by these mutations, and found it was not. Furthermore, Trm6p does not appear to play a role in AdoMet binding, as the *trm61-3* enzyme, which has wild-type Trm6p subunits, did not bind AdoMet.

Although heteroligomerization and AdoMet binding were not affected by the mutations we introduced, these mutants did exhibit strong defects in Mtase activity, which led us to discover that tRNA binding was compromised. This was an unexpected finding, considering that all of the mutated residues are predicted to be buried inside the protein and not exposed at the surface, where they could potentially interact with the tRNA substrate. In addition, our studies show that both Trm6p and Trm61p contribute to tRNA binding, as mutations in Trm61p alone abolished $tRNA_i^{Met}$ binding. Previous studies had shown that Trm61p could not bind $tRNA_i^{Met}$ without Trm6p, leading to the hypothesis that Trm6p is responsible for tRNA binding (10). However, the data presented here suggests that both subunits help to create the architecture necessary for substrate binding. We also observed that wild-type Trm6p/Trm61p complexes did not show an increased affinity for tRNA in the presence of S-adenosyl-L-homocysteine (data not shown). Similarly, the *trm61-3* enzyme, which cannot bind AdoMet, binds tRNA as efficiently as wild-type enzyme, suggesting that AdoMet binding is not required for tRNA binding. Finally, the K_d values for AdoMet and $tRNA_i^{Met}$ we report for the wild-type enzyme in this study are ~100-fold greater than the K_m values we reported previously, which were determined by measuring product formation in Mtase activity assays (10). It should be noted that these data are not contradictory, as K_d and K_m constants are not equivalent except in cases when the conversion of enzyme–substrate complexes to enzyme and product is a rate-limiting step. Since both K_d values are greater, we presume the conversion of enzyme–substrate to product is not a rate-limiting step.

Based on the crystal structure of TrmI, it was proposed that the tRNA substrate is bound in two clefts, one of which is found in the interface between the subunits and is lined with positively charged residues (12). We have calculated the electrostatic surface potential of the equivalent surface of the Trm6/Trm61p tetramer, and have found that it is negatively charged (Figure S2); however, the flexible extensions that are present in Trm6p and Trm61p but absent in TrmI (in particular regions comprising residues 265–345 in Trm61p and 455–478 in Trm6p, Figure S2) are positively charged. This suggests that the yeast m^1A58 Mtase uses a different mechanism for tRNA recognition and binding than its prokaryotic counterpart. Alternatively, the positively charged regions of Trm6p and Trm61p, which we cannot accurately position in our model, could be located in the interface between subunits. It would be interesting to determine whether or not the mutations that abolished tRNA

binding by the yeast Mtase would cause this same defect if present in TrmI.

Previously, it has been shown that the tRNA modification enzyme pseudouridine 55 synthase undergoes substantial conformation changes upon binding an RNA substrate (39). Unfortunately, the existing methodology does not allow modeling of large conformational changes, such as the induced fit of flexible protein loops upon the formation of a Mtase–tRNA complex. While the mutations we introduced into Trm6p and Trm61p are not exposed to the surface, they could bring about a conformational change of residues directly involved in tRNA binding. In the case of large systems such as Trm6p/Trm61p, modeling the conformational changes induced by the mutations we introduced would be speculative and time-consuming (in the order of years of calculations on a supercomputer), and is beyond the scope of this study. Therefore, we carried out only a preliminary assessment of the relative stability of the wild-type and mutated interface of Trm6p and Trm61p using the modeling system Sculpt (40). Sculpt optimizes intramolecular contacts to minimize the potential energy due to torsions, hydrogen bonds and van der Waals and electrostatic interactions, while constraining bond angles, bond lengths and dihedral angles (40). A wild-type Trm6p/Trm61p tetramer model or a model with E416, R420 and Y422 residues in Trm6p and E255, R259, and Y261 in Trm61p truncated beyond C_α atoms was subjected to energy minimization, with most of the molecule 'frozen', and only the regions 413–441 in Trm6p and 253–265 and 343–357 in Trm61p 'thawed' (data not shown). Using this analysis, which allowed the protein to shift to a minimum energy conformation, the structure of the mutant enzyme changed more than that of the wild-type enzyme, which changed very little. The backbone of the mutant protein is less stable because of the extra space created by the alanine substitutions, and because the interactions between side chains have been lost.

Although the above-mentioned simulation must be regarded as very preliminary and will have to be validated by more advanced computational methods and perhaps also by biophysical measurements, it generally agrees with our experimental finding that mutations of residues at the Trm6p/Trm61p interface do not disrupt oligomerization, but interfere with tRNA binding. Thus, we propose that the presence of salt bridges in the yeast m^1A58 Mtase (Trm61p-E255 and Trm6p-R420, and between Trm6p-E416 and Trm61p-R259), and most likely also in bacterial TrmI Mtases (e.g. E299-R233 in Rv2118c), serves to establish the structure of the tRNA-binding region rather than to promote binding of subunits to each other. We hypothesize that the mutations reported in this work could have long-range structural effects on the conformation of the positively charged loop (residues 265–345) in the Trm61p subunit, which may be involved in tRNA binding. By identifying amino acids involved in tRNA binding, this study has provided a foundation on which further studies can be built, such as experiments to address our hypothesis regarding tRNA binding and to determine how the yeast m^1A58 Mtase is able to recognize substrate tRNAs amongst the cellular tRNA pool.

ACKNOWLEDGEMENTS

We would like to thank Dr Glenn R. Björk and Kerstin Jacobsson for the HPLC analysis of modified nucleosides in tRNA. Glenn R. Björk is supported by grants from the Swedish Science Research Council (proj. B-BU 2930) and the Swedish Cancer Foundation (proj. 680). STD-NMR experiments were performed with the help of Dr Sheng Cai, Chemical Proteomics Facility, Marquette University. We thank Sarah L. Wassink for assistance with plasmid construction and protein purification. Sarah G. Ozanick was supported in part by a GAANN fellowship (Award No. P200A030199-05). This work was supported by NIGMS grant R15GM066791-01 to J.T.A. and NIH instrumentation grant S10RR019012 to D.S.S. Funding to pay the Open Access publication charges for this article was provided by NIGMS grant RO1GM069949 to JTA and GAAN fellowship award No. P200A030199-05.

Conflict of interest statement. None declared.

REFERENCES

1. Yarian,C., Townsend,H., Czestkowski,W., Sochacka,E., Malkiewicz,A.J., Guenther,R., Miskiewicz,A. and Agris,P.F. (2002) Accurate translation of the genetic code depends on tRNA modified nucleosides. *J. Biol. Chem.*, **277**, 16391–16395.
2. Urbonavičius,J., Qian,Q., Durand,J.M.B., Hagervall,T.G. and Björk,G.R. (2001) Improvement of reading frame maintenance is a common function for several tRNA modifications. *EMBO J.*, **20**, 4863–4873.
3. Madore,E., Florentz,C., Giege,R., Sekine,S., Yokoyama,S. and Lapointe,J. (1999) Effect of modified nucleotides on *Escherichia coli* tRNAGlu structure and on its aminoacylation by glutamyl-tRNA synthetase. Predominant and distinct roles of the mnm^5 and s^2 modifications of U34. *Eur. J. Biochem.*, **266**, 1128–1135.
4. Helm,M., Brule,H., Degoul,F., Cepanec,C., Leroux,J.P., Giege,R. and Florentz,C. (1998) The presence of modified nucleotides is required for cloverleaf folding of a human mitochondrial tRNA. *Nucleic Acids Res.*, **26**, 1636–1643.
5. Dunin-Horkawicz,S., Czerwoniec,A., Gajda,M.J., Feder,M., Grosjean,H. and Bujnicki,J.M. (2006) MODOMICS: a database of RNA modification pathways. *Nucleic Acids Res*, **34**, D145–D149.
6. Björk,G.R. (1995) In Söll,D. and RajBhandary,U.L. (eds), *tRNA: Structure Biosynthesis and Function*, ASM Press, pp. 165–206.
7. Anderson,J., Phan,L., Cuesta,R., Carlson,B.A., Pak,M., Asano,K., Bjork,G.R., Tamame,M. and Hinnebusch,A.G. (1998) The essential Gcd10p-Gcd14p nuclear complex is required for 1-methyladenosine modification and maturation of initiator methionyl-tRNA. *Genes Dev.*, **12**, 3650–3662.
8. Droogmans,L., Roovers,M., Bujnicki,J.M., Tricot,C., Hartsch,T., Stalon,V. and Grosjean,H. (2003) Cloning and characterization of tRNA (m^1A58) methyltransferase (TrmI) from Thermus thermophilus HB27, a protein required for cell growth at extreme temperatures. *Nucleic Acids Res.*, **31**, 2148–2156.
9. Roovers,M., Wouters,J., Bujnicki,J.M., Tricot,C., Stalon,V., Grosjean,H. and Droogmans,L. (2004) A primordial RNA modification enzyme: the case of tRNA (m^1A) methyltransferase. *Nucleic Acids Res.*, **32**, 465–476.
10. Anderson,J., Phan,L. and Hinnebusch,A.G. (2000) The Gcd10p/Gcd14p complex is the essential two-subunit tRNA(1-methyladenosine) methyltransferase of *Saccharomyces cerevisiae*. *Proc. Natl Acad. Sci. USA*, **97**, 5173–5178.

11. Ozanick,S., Krecic,A., Andersland,J. and Anderson,J.T. (2005) The bipartite structure of the tRNA m^1A58 methyltransferase from *S. cerevisiae* is conserved in humans. *RNA*, **11**, 1281–1290.
12. Gupta,A., Kumar,P.H., Dineshkumar,T.K., Varshney,U. and Subramanya,H.S. (2001) Crystal structure of Rv2118c: an AdoMet-dependent methyltransferase from *Mycobacterium tuberculosis* H37Rv. *J. Mol. Biol*, **312**, 381–391.
13. Bujnicki,J.M. (2001) In silico analysis of the tRNA:m^1A58 methyltransferase family: homology-based fold prediction and identification of new members from Eubacteria and Archaea. *FEBS Lett*, **507**, 123–127.
14. Li,J.N. and Bjork,G.R. (1999) Structural alterations of the tRNA(m^1G37)methyltransferase from *Salmonella typhimurium* affect tRNA substrate specificity. *RNA*, **5**, 395–408.
15. Watanabe,K., Nureki,O., Fukai,S., Endo,Y. and Hori,H. (2006) Functional categorization of the conserved basic amino acid residues in TrmH (tRNA (Gm18) methyltansferase) enzymes. *J. Biol. Chem*, **281**, 34630–34639.
16. Purta,E., van Vliet,F., Tricot,C., De Bie,L.G., Feder,M., Skowronek,K., Droogmans,L. and Bujnicki,J.M. (2005) Sequence-structure-function relationships of a tRNA (m^7G46) methyltransferase studied by homology modeling and site-directed mutagenesis. *Proteins*, **59**, 482–488.
17. Ahn,H.J., Kim,H.W., Yoon,H.J., Lee,B.I., Suh,S.W. and Yang,J.K. (2003) Crystal structure of the tRNA(m^1G37) methyltransferase: insights into tRNA recognition. *EMBO J*, **22**, 2593–2603.
18. Nureki,O., Watanabe,K., Fukai,S., Ishii,R., Endo,Y., Hori,H. and Yokoyama,S. (2004) Deep knot structure for construction of active site and cofactor binding site of tRNA modification enzyme. *Structure*, **12**, 593–602.
19. Zegers,I., Gigot,D., Van Vliet,F., Tricot,C., Aymerich,S., Bujnicki,J.M., Kosinski,J. and Droogmans,L. (2006) Crystal structure of *Bacillus subtilis* TrmB, the tRNA (m^7G46) methyltransferase. *Nucleic Acids Res*, **34**, 1925–1934.
20. Johansson,M.J.O. and Bystrom,A.S. (2005) In Grosjean,H. (ed), *Fine-Tuning of RNA Functions by Modification and Editing*, Springer-Verlag, Berlin, Vol. 12, pp. 87–120.
21. Hopper,A.K. and Phizicky,E.M. (2003) tRNA transfers to the limelight. *Genes Dev*, **17**, 162–180.
22. Schubert,H.L., Blumenthal,R.M. and Cheng,X. (2003) Many paths to methyltransfer: a chronicle of convergence. *Trends Biochem. Sci*, **28**, 329–335.
23. Dever,T.E., Yang,W., Åström,S., Byström,A.S. and Hinnebusch,A.G. (1995) Modulation of $tRNA_i^{Met}$, eIF-2 and eIF-2B expression shows that *GCN4* translation is inversely coupled to the level of eIF-2GTP Met-$tRNA_i^{Met}$ ternary complexes. *Mol. Cell. Biol*, **15**, 6351–6363.
24. Ito,H., Fukada,Y., Murata,K. and Kimura,A. (1983) Transformation of intact yeast cells treated with alkali cations. *J. Bacteriol*, **153**, 163–168.
25. Gietz,R.D. and Sugino,A. (1988) New yeast-*Escherichia coli* shuttle vectors constructed with *in vitro* mutagenized yeast genes lacking six-base pair restriction sites. *Gene*, **74**, 527–534.
26. Cuesta,R., Hinnebusch,A.G. and Tamame,M. (1998) Identification of *GCD14* and *GCD15*, novel genes required for translational repression of *GCN4* mRNA in *Saccharomyces cerevisiae*. *Genetics*, **148**, 1007–1020.
27. Sikorski,R.S. and Hieter,P. (1989) A system of shuttle vectors and yeast host strains designed for efficient manipulation of DNA in *Saccharomyces cerevisiae*. *Genetics*, **122**, 19–27.
28. Garcia-Barrio,M.T., Naranda,T., Cuesta,R., Hinnebusch,A.G., Hershey,J.W.B. and Tamame,M. (1995) GCD10, a translational repressor of *GCN4*, is the RNA-binding subunit of eukaryotic translation initiation factor-3. *Genes Dev*, **9**, 1781–1796.
29. Kurowski,M.A. and Bujnicki,J.M. (2003) GeneSilico protein structure prediction meta-server. *Nucleic Acids Res*, **31**, 3305–3307.
30. Kosinski,J., Cymerman,I.A., Feder,M., Kurowski,M.A., Sasin,J.M. and Bujnicki,J.M. (2003) A ''FRankenstein's monster'' approach to comparative modeling: merging the finest fragments of fold-recognition models and iterative model refinement aided by 3D structure evaluation. *Proteins*, **53**(Suppl 6), 369–379.
31. Maniatis,T., Fritsch,E.F. and Sambrook,J. (1982) *Molecular Cloning: a Laboratory Manual*. Cold Spring Harbor Laboratory Press, Cold Spring Harbor, NY.
32. Stockman,B.J. and Dalvit,C. (2002) NMR screening techniques in drug discovery and drug design. *Prog. NMR Spectroscopy*, **41**, 187–231.
33. Harashima,S. and Hinnebusch,A.G. (1986) Multiple *GCD* genes required for repression of *GCN4*, a transcriptional activator of amino acid biosynthetic genes in *Saccharomyces cerevisiae*. *Mol. Cell Biol*, **6**, 3990–3998.
34. Calvo,O., Cuesta,R., Anderson,J., Gutierrez,N., Garcia-Barrio,M.T., Hinnebusch,A.G. and Tamame,M. (1999) GCD14p, a repressor of *GCN4* translation, cooperates with Gcd10p and Lhp1p in the maturation of initiator methionyl-tRNA in *Saccharomyces cerevisiae*. *Mol. Cell. Biol*, **19**, 4167–4181.
35. Jiang,H.Q., Motorin,Y., Jin,Y.X. and Grosjean,H. (1997) Pleiotropic effects of intron removal on base modification pattern of yeast tRNAPhe: an *in vitro* study. *Nucleic Acids Res*, **25**, 2694–2701.
36. Sem,D.S. (2006) *NMR-guided Fragment Assembly*. Wiley-VCH, Weinheim, Germany.
37. Mayer,M. and Meyer,B. (1999) Characterization of ligand binding by saturation transfer difference NMR spectroscopy. *Angew. Chem. Int. Ed*, **38**, 1784–1788.
38. Hanna,G.M. (2004) NMR regulatory analysis: determination and characterization of S-adenosyl-L-methionine in dietary supplements. *Pharmazie*, **59**, 251–256.
39. Phannachet,K. and Huang,R.H. (2004) Conformational change of pseudouridine 55 synthase upon its association with RNA substrate. *Nucleic Acids Res*, **32**, 1422–1429.
40. Surles,M.C., Richardson,J.S., Richardson,D.C. and Brooks,F.P. Jr. (1994) Sculpting proteins interactively: continual energy minimization embedded in a graphical modeling system. *Protein Sci*, **3**, 198–210.
41. DeLano,W.L. (2002) DeLano Scientific. *The PyMOL Molecular Graphics System* Palo Alto, CA, USA.